

Artificial bee colony based state feedback position controller for PMSM servo-drive – the efficiency analysis

T. TARCZEWSKI^{1*}, L.J. NIEWIARA¹, and L.M. GRZESIAK²

¹Institute of Engineering and Technology, Nicolaus Copernicus University, ul. Grudziądzka 5, 87-100 Torun, Poland

²Institute of Control and Industrial Electronics, Warsaw University of Technology, ul. Koszykowa 75, 00-662 Warsaw, Poland

Abstract. This paper presents a state feedback controller (SFC) for position control of PMSM servo-drive. Firstly, a short review of the commonly used swarm-based optimization algorithms for tuning of SFC is presented. Then designing process of current control loop as well as of SFC with feedforward path is depicted. Next, coefficients of controller are tuned by using an artificial bee colony (ABC) optimization algorithm. Three of the most commonly applied tuning methods (i.e. linear-quadratic optimization, pole placement technique and direct selection of coefficients) are used and investigated in terms of positioning performance, disturbance compensation and robustness against plant parameter changes. Simulation analysis is supported by experimental tests conducted on laboratory stand with modern PMSM servo-drive.

Key words: tuning, PMSM servo-drive, artificial bee colony algorithm, linear-quadratic optimization, pole placement.

1. Introduction

Nowadays, servo-drives with PMSM are commonly applied in motion control applications such as industrial robots or CNC machines [1–3]. It is caused by superior dynamic properties, high torque to inertia ratio, reliability and effectiveness of PMSM [4–7]. In order to achieve high-performance position control of servo-drive, advanced control schemes are applied to regulate mechanical variables (i.e. angular position and velocity). For example, in [8] a nonlinear H_∞ control scheme is proposed for PMSM servo-drive. In this solution, sliding mode control (SMC) is used to improve robustness against parameter variations. As a result, an efficient robust position controller for PMSM is obtained, however, selection procedure of the controller parameters for H_∞ is made manually which requires expert knowledge and seems to be difficult. As it was reported in [9], the selection process of SMC parameters has a direct impact on control performance and it may be supported by evolutionary algorithm. In this approach differential evolution (DE) algorithm has been used to optimize parameters of SMC. It was proven that the application of DE improves performance and robustness of servo system. As it was shown in [10], neural network based adaptive controller may also be applied to control PMSM servo-drive. The experimental results confirm that the proposed solution assures robust tracking performance in the case of parameter uncertainties. Similarly to the solution presented above, several coefficients are designed manually to provide the best performance. Another approach related to position tracking of PMSM servo-drive is based on iterative learn-

ing control (ILC) [11]. In this solution, a state feedback controller (SFC) with integral path is incorporated with ILC law to ensure the reduction of steady-state position error caused by a load torque. Although designing process of SFC was supported by Matlab toolboxes (i.e. CVX, SDPT3), weighting matrices needed for minimization of the quadratic cost function have been chosen manually. Presented results confirm that the proposed control scheme is capable of achieving small tracking errors after a small number of iterations.

As it was shown in [12, 13] an application of SFC assures nonlinearity tolerance and robustness. Moreover, the computational effort of constrained SFC is relatively low and it can be implemented in a modern (e.g. SiC based) servo-drive, where time available for execution of control algorithm is limited due to high switching and sampling frequencies ($f_s > 20$ kHz) [14]. In such a case, quiet and efficient operation of PMSM servo-drive can be obtained. Since all coefficients of SFC must be selected simultaneously, synthesis procedure is not trivial. In the case of manual tuning of SFC, a linear-quadratic optimization method and a pole placement technique are most often applied [15, 16]. Even for these approaches tuning process is still complex and it requires expert knowledge usually supported by many time consuming attempts.

The above-mentioned disadvantage causes that automatic selection of SFC coefficients is gaining attention. Swarm-based optimization algorithms are also employed in this field because of good convergence and efficiency. From the literature review, one can conclude that regardless of optimization algorithm used (e.g. genetic algorithm – GA, particle swarm optimization – PSO, artificial bee colony – ABC) in most cases coefficients of SFC are calculated with the help of linear-quadratic optimization. In such a case, optimization algorithm is utilized to find optimal values of weighting matrices needed for calculation of SFC. For example in [17], PSO is em-

*e-mail: ttarczewski@umk.pl

Manuscript submitted 2020-01-09, revised 2020-03-20, initially accepted for publication 2020-04-11, published in October 2020

ployed to obtain weighting matrices of linear-quadratic regulator (LQR) designed for IPMSM drive. The presented results demonstrate the feasibility of the proposed approach, however, the introduction of constraints on state variables (i.e. dq axes currents) is not considered. In [18], GA is applied to design weighting matrices of LQR for multimachine power system. In this study a better control performance of GA-LQR has been reported in comparison to LQR with manually selected weighting matrices. In the proposed approach the introduction of constraints is not taken into account. As it was shown in [19], a relatively novel nature-inspired artificial bee colony optimization algorithm can also be applied to tuning process of LQR designed for PMSM servo-drive. Contrary to solutions described above, constraints handling method has been incorporated with optimization scheme to provide limitation of state variables. As a result, safe operation of the servo-drive can be achieved. In [20], comparison between LQR and pole placement technique for flexible link manipulator is shown. Since the pole placement is made with the help of PSO while weighting matrices for LQR are selected manually, inference about the effectiveness of applied methods is not possible.

In this paper, three of the most commonly employed tuning methods (i.e. linear-quadratic optimization, pole placement technique and direct selection of coefficients) are implemented in tuning procedure supported by ABC optimization algorithm. Designed controller is applied to motion control of modern PMSM servo-drive. The efficiency of state feedback controller based on ABC is investigated in terms of positioning performance, disturbance compensation and robustness against plant parameter changes. The initial version of this concept was presented in [21]. In this paper, further information concerning the control structure, optimization algorithm as well as the literature review in a field of complex motion control schemes supported by nature-inspired optimization methods are depicted.

The rest of the paper is organized as follows. Section 2 describes the proposed control structure with respect to model of the servo-drive, current control loop, and motion control state feedback controller. In Section 3, based on ABC tuning of SFC is presented. Section 4 demonstrates numerical experiments, including repeatability, convergence, real-time responses of the servo-drive as well as robustness. Finally, Section 5 concludes this paper.

2. Mathematical model of the drive and the control structure

Block diagram of the considered control structure is presented in Fig. 1. In this approach space vector components of the PMSM currents are regulated using PI controllers, while mechanical variables of the servo-drive (i.e. angular velocity and position) are controlled using state feedback controller. In order to improve the load torque compensation, the feedforward path from estimated load torque has been introduced along with the load torque observer.

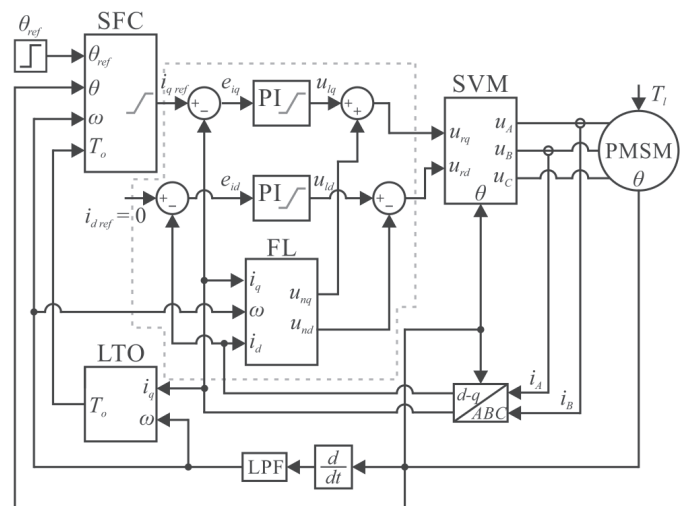


Fig. 1. Block diagram of the control structure with PMSM servo-drive: SFC - state feedback controller, LTO – load torque observer, FL – feedback linearization, PI – current controller, SVM – space vector modulator, PMSM – permanent magnet synchronous motor, LPF – low pass filter

2.1. Current control loop. During synthesis process of the current control loop several simplifying assumptions related to the electrical part of the servo-drive have been made. Firstly, dynamics and nonlinearities of the VSI have been omitted. Since SiC based power semiconductors were utilized and power converter operates in a linear range above-mentioned assumptions are valid. Secondly, it was also assumed that PMSM with surface mounted magnets is considered and in this particular case inductances in dq axes are equal (i.e. $L_d = L_q = L_s$). Finally, it is well-known that the model of the electrical part of the PMSM is nonlinear and cross-coupled [22]. To overcome this disadvantage a feedback linearization method has been applied and current controllers were designed for linear model of the plant described by the following formulas [19]:

$$u_{rd}(t) = u_{ld}(t)K_p + u_{nd}(t)K_p = R_s i_d(t) + L_s \frac{di_d(t)}{dt}, \quad (1)$$

$$u_{rq}(t) = u_{lq}(t)K_p + u_{nq}(t)K_p = R_s i_q(t) + L_s \frac{di_q(t)}{dt} \quad (2)$$

with:

$$u_{nd}(t) = p\omega(t)L_s i_q(t)/K_p, \quad (3)$$

$$u_{nq}(t) = -p\omega(t)(L_s i_d(t) + \psi_f)/K_p, \quad (4)$$

where: $u_{ld}(t)$, $u_{lq}(t)$ and $u_{nd}(t)$, $u_{nq}(t)$ – linear and nonlinear space vector components of voltages, $u_{rd}(t)$, $u_{rq}(t)$ – input space vector components of SVM, K_p – gain of VSI, R_s – stator resistance, $\omega(t)$ – angular velocity, $i_d(t)$, $i_q(t)$ – current space vector components. From (1)–(2) one can see that the right hand sides are linear and these will be applied during synthesis process of the PI current controllers. However, nonlinear and cross-coupled terms are included in $u_{nd}(t)$, $u_{nq}(t)$ and these

will be added to the respective signals produced by controllers, which was shown in Fig. 2.

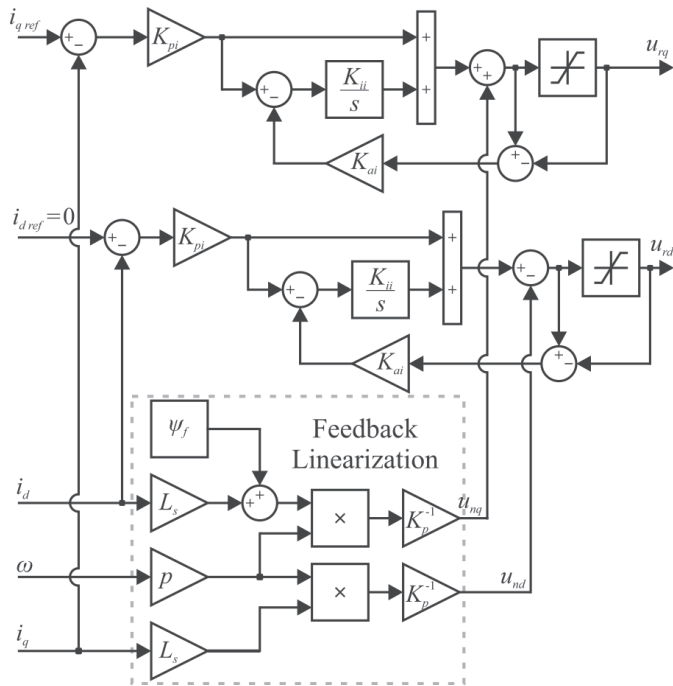


Fig. 2. Current controllers with feedback linearization

Tuning procedure of PI current controllers has been made by using an internal model control (IMC) method [23]. In this approach required rise time of controlled variable (dq -axis currents in this particular case) is used to calculate coefficients of controller. The following formulas are applied:

$$K_{pi} = \alpha L_s / K_p, \tag{5}$$

$$K_{ii} = R_s / L_s, \tag{6}$$

where: $\alpha = \log(9) / \tau_{ri}$, τ_{ri} – the required rise time of current. Finally, from Fig. 2 one can see that an anti-windup path based on the tracking back calculation approach has been adopted [24].

2.2. Control of mechanical variables. Synthesis process of state feedback controller for angular position and velocity requires a state equation of servo-drive mechanical part. Several assumptions have been made during the considered procedure. Firstly, the dynamics of current control loop is omitted, which is consistent with the theory related to electrical drives [19, 25]. Secondly, the load torque is treated as an external disturbance and therefore it will be omitted in synthesis procedure. However, an additional feedforward path will be introduced to improve load torque compensation. Finally, to provide steady-state error-free operation of servo-drive, state equation will be augmented by additional state variable. The above-mentioned state equation has the following form:

$$\frac{d\mathbf{x}(t)}{dt} = \mathbf{A}\mathbf{x}(t) + \mathbf{B}u(t) + \mathbf{F}r(t), \tag{7}$$

with:

$$\mathbf{x}(t) = \begin{bmatrix} \omega(t) \\ \theta(t) \\ e_\theta \end{bmatrix}, \quad \mathbf{A} = \begin{bmatrix} -\frac{B_m}{J_m} & 0 & 0 \\ 1 & 0 & 0 \\ 0 & 1 & 0 \end{bmatrix}, \quad \mathbf{B} = \begin{bmatrix} \frac{K_t}{J_m} \\ 0 \\ 0 \end{bmatrix},$$

$$u(t) = i_{qref}(t), \quad \mathbf{F}^T = [0 \quad 0 \quad -1], \quad r(t) = \theta_{ref}(t),$$

where: $\theta(t)$ – angular position of the motor shaft, B_m – viscous friction, J_m – moment of inertia, K_t – torque constant, $\theta_{ref}(t)$ – reference position, $i_{qref}(t)$ – reference value of q -axis component. It is worth noting that the last state variable $e_\theta(t)$ from (7) conforms to the integral of angular position error:

$$e_\theta(t) = \int_0^t [\theta(\tau) - \theta_{ref}(\tau)] d\tau. \tag{8}$$

This assures steady-state error-free operation of servo-drive for step changes of $\theta_{ref}(t)$ and load torque, respectively.

For state feedback controller designed to control mechanical state variables of the servo-drive (i.e. $\omega(t)$, $\theta(t)$, $e_\theta(t)$), the following control law will be obtained for the state equation (7):

$$u(t) = -\mathbf{K}\mathbf{x}(t), \tag{9}$$

where: $\mathbf{K} = [k_1 \quad k_2 \quad k_3]$ – gain matrix of considered controller.

As it was mentioned earlier, the load torque has not been considered during designing of SFC. However, its impact on the control performance may be limited if a feedforward path is introduced. In such a case, modified control law takes the following form:

$$u(t) = -\mathbf{K}\mathbf{x}(t) - k_f d(t), \tag{10}$$

where: k_f – the feedforward coefficient, $d = T_o$ – estimated value of the load torque. In order to obtain the value of the k_f , a residual model (i.e. constructed for deviations from steady state) of the control system should be developed [26, 27]. For a control system described by the state equation (7) and the control law (9) the residual model is as follows:

$$k_f = [\mathbf{K}_x \quad 1] \mathbf{G}^{-1} \mathbf{E} \tag{11}$$

with:

$$\mathbf{K}_x = [k_1 \quad k_2], \quad \mathbf{G} = [\mathbf{A}_x \quad \mathbf{B}_x],$$

$$\mathbf{E} = \begin{bmatrix} -\frac{1}{J_m} \\ 0 \end{bmatrix}, \quad \mathbf{A}_x = \begin{bmatrix} -\frac{B_m}{J_m} & 0 \\ 1 & 0 \end{bmatrix}, \quad \mathbf{B}_x = \begin{bmatrix} \frac{K_t}{J_m} \\ 0 \end{bmatrix}.$$

Block diagram of the proposed state feedback position controller with feedforward path described by the control law (10) is illustrated in Fig. 3.

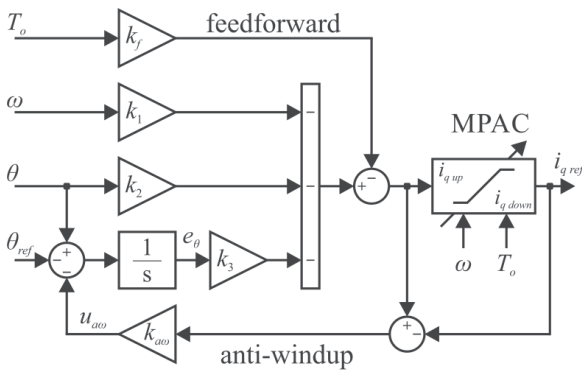


Fig. 3. Block diagram of state feedback position controller with feedforward path and MPAC

From the block diagram shown in Fig. 3 one can see that two additional parts not considered in the control law (10) have been included. Firstly, model predictive approach to constraints (MPAC) introduction was added. It is responsible for imposing constraints on internal state variable (i.e. ω) as well as on the output variable (i.e. i_{qref}) of considered control system. In this concept a discrete predictive formula based on the mechanical equation of the PMSM is utilized to keep selected variables in a desired ranges. Detailed information about MPAC can be found in [14, 19]. The task related to imposing constraints into cascade-free motion control system may also be done using barrier Lyapunov functions approach [28] and nonlinear state transformation method [29]. Secondly, after the introduction of MPAC, designed control system operates with limited control signal. Since an integral path is present in SFC, the above-mentioned limitation may cause a windup phenomenon. To overcome this, an anti-windup path based on the tracking back calculation approach has been adopted [24]. Finally, actual value of the load torque is required in a controller shown in Fig. 3. It is utilized in a feedforward path as well as in MPAC. Since the load torque is treated as nonmeasurable disturbance, it was decided to implement the load torque observer based on a typical Luenberger structure. Information related to designing and tuning procedures of such an observer can be found in [30].

As it was previously mentioned, the selection process of SFC coefficients is not trivial. Since the considered procedure requires expert knowledge usually supported by many time consuming attempts, it can be supported by optimization algorithm. In this particular case it was decided to utilize nature-inspired optimization method due to its advantages depicted in the next section.

3. Tuning of state feedback controller

Recently, nature-inspired swarm-based optimization algorithms are increasingly applied to tuning of complex controllers in a motion control field [17–20, 25]. In the case of state feedback controller, similarly to manual tuning, automatic selection can be done using direct selection, pole placement or linear-quadratic optimization. Due to this it was decided to investigate

the efficiency of tuning process for the above-mentioned tuning methods.

Among all swarm based optimization schemes, the artificial bee colony optimization algorithm was selected because of superior convergence and possibility of incorporating parameter-free constraints handling method. The last advantage is substantial in this particular case since tuned controller is responsible for safe and proper operation of the servo-drive. A very good convergence of ABC is related to the more complex searching process in comparison to the most popular optimization schemes (e.g. PSO). In ABC the colony is divided into three groups responsible for: global, local and random searching in the solution space. It is worth pointing out that information about the quality of solution is shared between global and local searching (i.e. employed bees inform onlookers about the fitness of explored food source). At this stage constraints handling method (e.g. Deb's rule, augmented Lagrangian [31]) is applied to favour the solution that does not exceed the specified limits. In the case of the servo-drive with considered control structure, safe operation requires limitation of the angular velocity and the reference current in q -axis, respectively. Flowchart of ABC optimization algorithm is shown in Fig. 4.

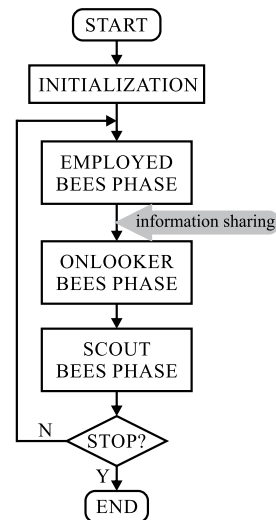


Fig. 4. Flowchart of ABC optimization algorithm

During initialization phase, random generation of optimized parameters is made. Next, in employed bees phase global searching process is realized. Temporary results of optimization are shared with onlooker bees phase to increase the number of bees that explore the solution space in the neighbourhood of the best solution. Finally, the scout bees phase is used for random searching. It runs if the employed bee cannot improve the quality of the solution in several attempts. The optimization scheme operates while the stop criteria is not full filled. In this particular case, the maximum number of iterations defines stop criteria.

The main parameters associated with ABC algorithm are: NP – the number of artificial bee colony size, FN – the number of food sources, D – the number of optimized parameters, MR modification ratio, $limit$ as well as lb – the lower and ub – the upper bounds of the search space. Typically, the number

of food sources is equal to the half of the colony: $FN = NP/2$. These values along with the modification ratio (typically equals to 0.8) are responsible for convergence. The *limit* parameter determines a number of attempts made by the employed bee during local search. The lower and the upper bounds are used to introduce constraints on the optimized parameters. This aspect will be discussed in the later part of the paper.

Supported by optimization algorithm tuning of state feedback controller requires determination of the performance index. Since constraints handling method is implemented in ABC, it is possible to construct a relatively simple, parameter-free performance index to fulfill satisfactory dynamic properties of servo-drive in the case of step changes of the reference position and the load torque as well as steady-state error-free operation. A discrete form of a performance index applied is as follows:

$$I_{ABC} = \sum_{n=0}^N |\theta_{ref}(n) - \theta(n)| nT_s, \quad (12)$$

where: T_s – the sampling period, N – the number of samples per reference signal.

As it was previously said, automatic selection of SFC coefficients will be made by using: (i) direct selection, (ii) pole placement and, (iii) linear-quadratic optimization. In the case of the last approach, the ABC algorithm was applied to determine the values of weighting matrices that minimize the following discrete performance index:

$$I_{LQR} = \sum_{n=0}^{\infty} [\mathbf{x}^T(n)\mathbf{Q}\mathbf{x}(n) + u^2(n)R] \quad (13)$$

with:

$$\mathbf{Q} = \text{diag} \left(\begin{bmatrix} q_1 & q_2 & q_3 \end{bmatrix} \right), \quad R, \quad (14)$$

where: q_i , R – coefficients of weighting matrices. Values of above-mentioned weighting matrices have been selected by ABC optimization algorithm and utilized in `lqr` function from Matlab Control System Toolbox (CST) to obtain SFC coefficients. Since it is necessary to bound solution space in ABC, values of weighting matrices for considered approach were limited to the range $(1 \times 10^{-6}; 1 \times 10^6)$.

In the case of pole placement technique, the rank of a state matrix in (7) determines the number of poles. Since control of mechanical variables of servo-drive is considered, it is advisable to provide step response without overshoot. Due to this, it was decided to decline complex poles and to limit the solution space to the following range: $(-30 + \delta; -1 \times 10^{-3})$. Since the `place` command cannot locate poles with multiplicity greater than $\text{rank}(B)$, an additional coefficient $\delta \in \{-0.1; 0; 0.1\}$ was introduced.

For direct selection of SFC's coefficients, it was decided to bound the range of potential solutions to the following set: $k_i \in (1 \times 10^{-2}; 1 \times 10^2)$. It should be noted that bounds for all considered approaches were set relatively wide to ensure free selection of optimized parameters. Moreover, a possibility of obtaining similar SFC's coefficients for all methods was also taken into account.

4. Numerical analysis and real-world experiments

4.1. Tuning of SFC. The ABC based selection of SFC's coefficients has been made for three methods. Constrained optimization algorithm described in a former section has been applied for selection of: (i) weighting matrices for linear-quadratic optimization, (ii) pole placement and, (iii) gain coefficients of controller. In all cases tuning procedure was made in Matlab/Simulink environment. Selected parameters of investigated PMSM servo-drive are listed in Table 1, while control parameters of ABC are summarized in Table 2.

Table 1
Selected parameters of servo-drive

Parameter	Symbol	Unit	Value
Rated angular velocity	ω_N	rad/s	50
Rated current	i_N	A	5
Moment of inertia	J_m	kg · m ²	8.6×10^{-3}
Viscous friction	B_m	N · m · s/rad	1.4×10^{-2}
Torque constant	K_t	N · m/A	1.14
Switching frequency	f_s	kHz	22

Table 2
Selected parameters of ABC

Parameter	Symbol	Value
Number of optimized parameters	D	3 v 4
Colony size	NP	20
Number of food sources	FN	$NP/2$
Maximum number of cycles	MCN	50
Control parameter	<i>limit</i>	$FN \times D$
Scout production period	<i>SPP</i>	$FN \times D$
Modification ratio	<i>MR</i>	0.8

From Table 2 one can see that the colony size has a direct impact on several parameters. As it was previously mentioned, the modification ratio *MR* is responsible for convergence and its value was selected according to information contained in [32].

During automatic selection of SFC's coefficients the following assumptions have been made: (i) minimization of (12), limitation of $|i| \leq 5A$ and $|\omega| \leq 50$ rad/s. It should be noted that at this stage MPAC implemented on the output of the SFC (see Fig. 3) remains inactive and constraints handling method implemented in ABC is responsible for the safe operation of the servo-drive.

Tuning was made for step change of the reference position $\theta_{ref} = 2\pi$ rad at $t = 0$ s along with step change of the load torque $T_l = 3$ N · m for $t \in (0.3; 0.4)$ s. Three considered tuning methods have been carried out in 10 independent runs to investigate repeatability. The total time needed to accomplish

single run (i.e. 50 iterations) is approx. 20 minutes and it is mainly consumed by the simulation of control system in Matlab/Simulink. Final values of the performance index I_{ABC} (12) obtained for the considered approaches are shown in Fig. 5.

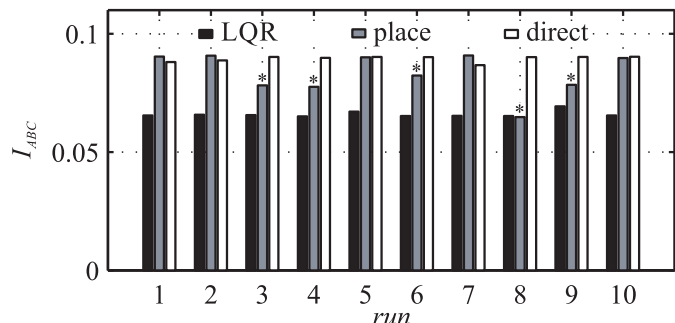


Fig. 5. Performance index (12) obtained after 10 runs

From Fig. 5 one can see that the lowest values of the performance index were obtained for linear-quadratic optimization method. In the case of the pole placement technique only half of the solutions meet requirements related to keeping the q -axis current and the angular velocity in desired ranges. Those that do not keep selected variables below limits were marked with the asterisk in Fig. 5 and will be omitted in experimental tests. Finally, results obtained for direct tuning of SFC assure proper limitation of the q -axis current and the angular velocity, however, values of I_{ABC} are higher in comparison to LQR.

SFC's coefficients obtained in each tuning process are shown in Fig. 6. It is observed that the lowest values of considered coefficients are obtained for LQR technique. Moreover, deviation of coefficients calculated for 10 runs is also smallest for the considered approach. Since linear-quadratic approach utilizes optimization during the selection of weighting matrices, its application to tuning procedure ensures better performance indexes in comparison to pole placement technique and direct selection. Values of unbiased standard deviation are listed in Table 3.

Table 3
An unbiased standard deviation of SFC coefficients

Coefficient	LQR	place*	direct
k_1	0.0038	0.0135	0.1339
k_2	0.1398	0.4557	2.3079
k_3	1.2045	3.3403	17.2994

From the obtained results it may be concluded that application of LQR in ABC based tuning procedure provides the most repeatable results. Regardless of tuning method, k_3 coefficient reaches the highest values, which is typical in control systems with SFC [19, 20].

In the next stage of studies, SFCs with the smallest performance indexes obtained for three considered approaches have been investigated. The evolution of the performance index recorded for the best run from each 10 attempts is shown

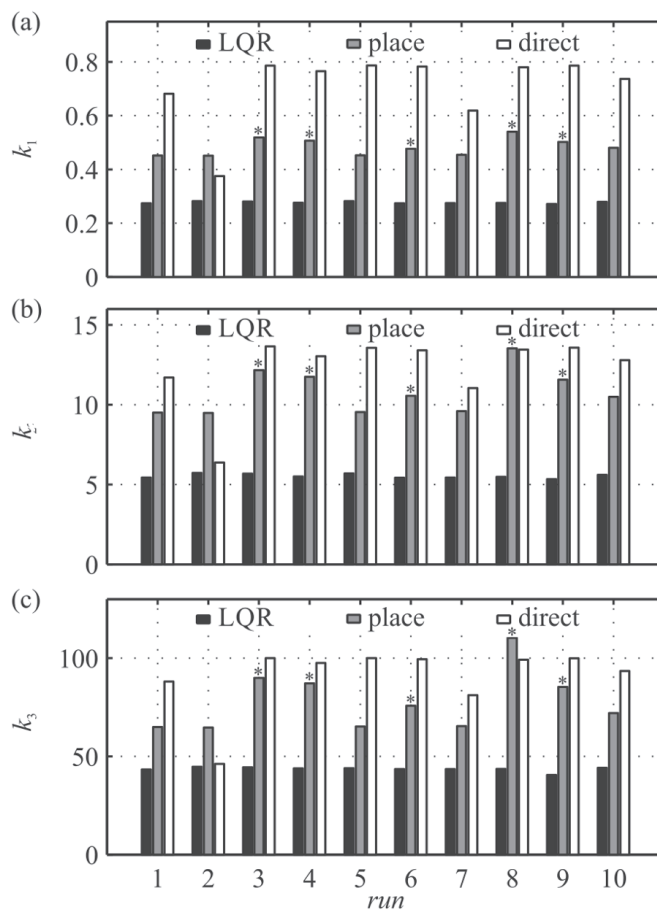


Fig. 6. Coefficients of SFC obtained after 10 runs

at the top of Fig. 8. For LQR and direct selection of coefficients the performance index reaches a steady-state after 25-th iteration. In the case of pole placement approach, the performance index remains constant during optimization process observed for the best run. For the comparison purposes evolution of the second best performance index has also been presented. Its value changes slightly after 17-th iteration. Evolution of the servo-drive angular position is presented at the bottom of Fig. 8. Since initial coefficients are randomly selected, quite different responses of the servo-drive for the first iteration are obtained, however, after 20 iterations a good position tracking as well as satisfactory load torque compensation has been achieved. The final values of the performance index as well as of SFC coefficients are summarized in Table 4. It should be noted that the

Table 4
Final values of I_{ABC} and SFC coefficients

	LQR	place*	direct
$I_{ABC\ best}$	0.0651	0.0898	0.0881
$k_{1\ best}$	0.2758	0.4805	0.6815
$k_{2\ best}$	5.4998	10.4841	11.6979
$k_{3\ best}$	43.8481	73.0032	88.029

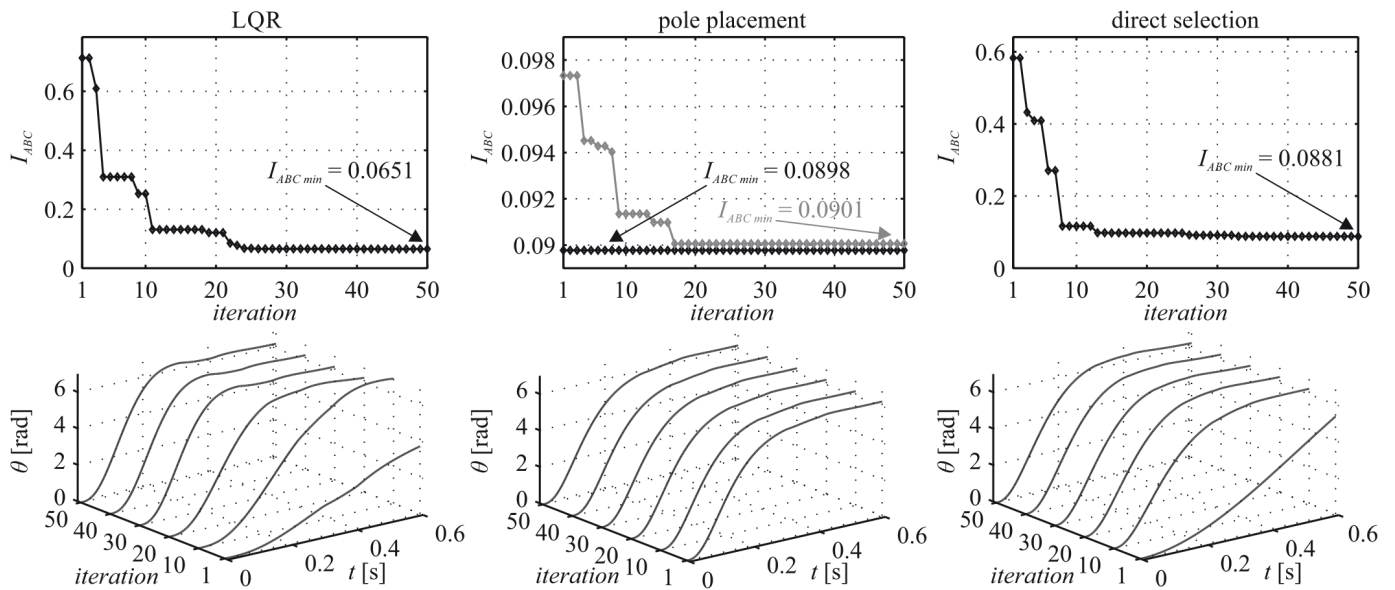


Fig. 8. Evolution of performance index (top) and angular position (bottom) during tuning

lowest value of I_{ABC} was obtained for LQR regardless of the lowest coefficients of the controller. It is caused by additional optimization applied for the selection of weighting matrices. Finally, it should be noted that the value of feedforward coefficient is independent on the SFC and it is equal to $k_f = -0.8736$.

4.2. Experimental responses. The performance of SFC with coefficients selected using ABC for three above mentioned methods has been investigated on a modern prototype PMSM servo-drive with SiC MOSFETs power semiconductors. Designed control algorithm was implemented in ST32F4 microcontroller. Since modern power stage and control device has been used, it was possible to set a relatively high sampling and switching frequencies $f_s = 22$ kHz. The laboratory stand consists of investigated servo-drive, the load drive and an additional moment of inertia. The load motor is controlled by commercial drive and it is used to impose load torque of the main servo-drive shaft. More detailed information related to the prototype servo-drive can be found in [33] while the photo of laboratory stand is shown in Fig. 7.

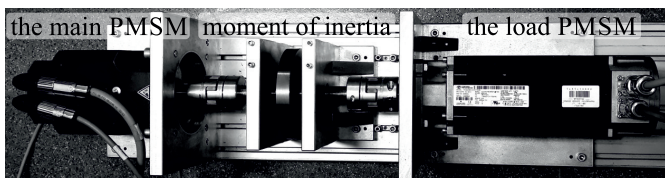


Fig. 7. Photo of laboratory stand

Firstly, the current control loop has been investigated and q -axis current step responses recorded for the angular velocity equal to zero are shown in Fig. 9. Since a relatively high switching frequency is used, it was possible to obtain a rise time of q -axis current at the level of $\tau_{ri} = 0.5$ ms. From Fig. 9 one can

see good dynamical properties of servo-drive electrical part as well as proper operation with zero d -axis current.

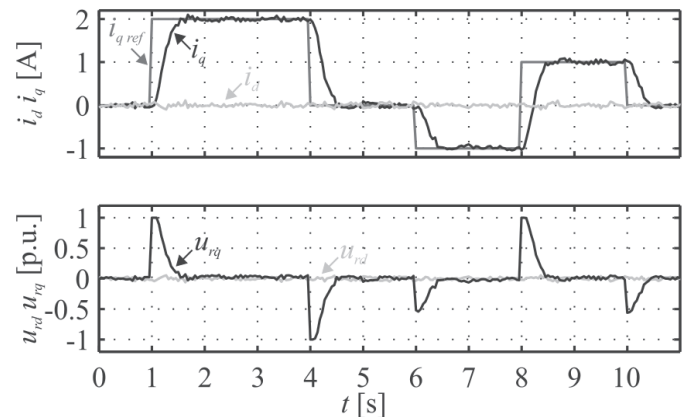


Fig. 9. Experimental responses of the current control loop

Next, SFC responsible for control of servo-drive mechanical variables was investigated and responses to step changes of angular position are presented in Fig. 10. It can be seen that the best dynamic properties are obtained for the controller based on linear-quadratic optimization. In the case of direct selection of SFC's coefficients an overshoot of angular position is observed. Since only negative real values of poles may be chosen by ABC optimization algorithm during tuning, an overshoot of the angular position is not observed in this approach. Proper limitation of the q -axis current proves the ability of constrained ABC optimization algorithm to tuning of servo-drive controller. However, as it was indicated earlier, only half of solutions obtained for the pole placement technique meet requirements related to keeping selected variables in admissible ranges. To solve this issue a wider area for poles location should be defined or complex poles should be permitted.

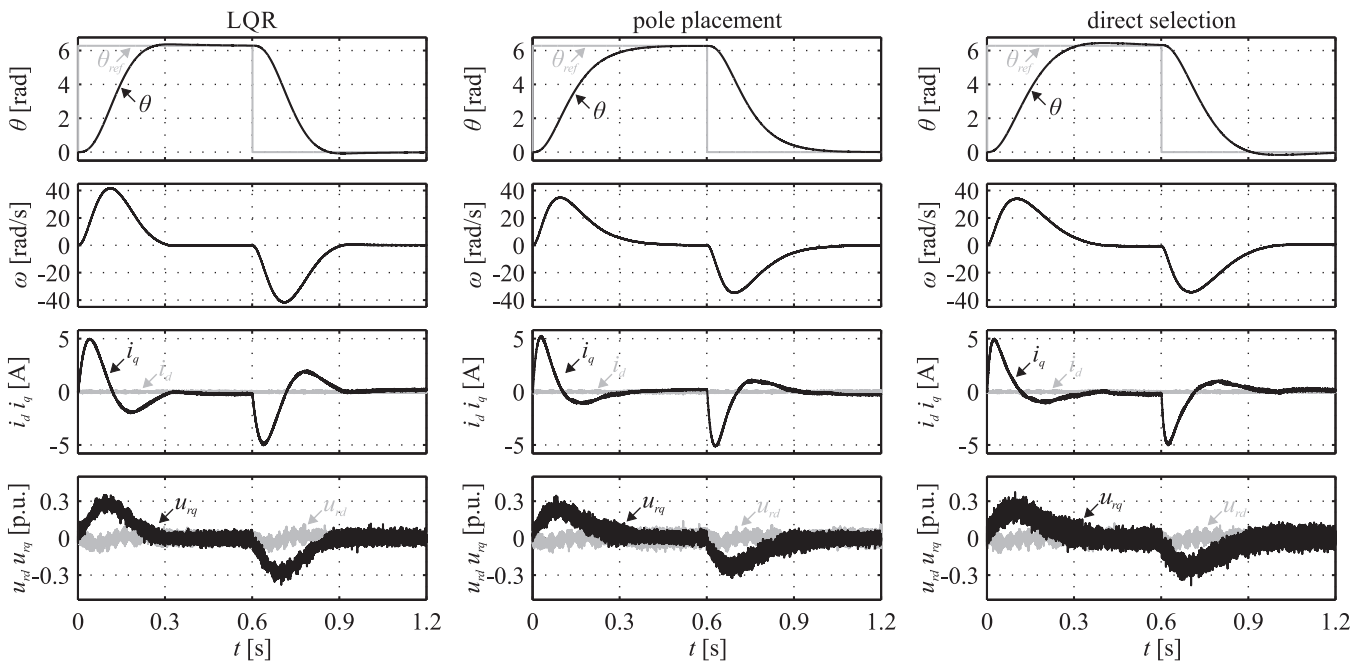


Fig. 10. Experimental responses of PMSM servo-drive to step changes of angular position

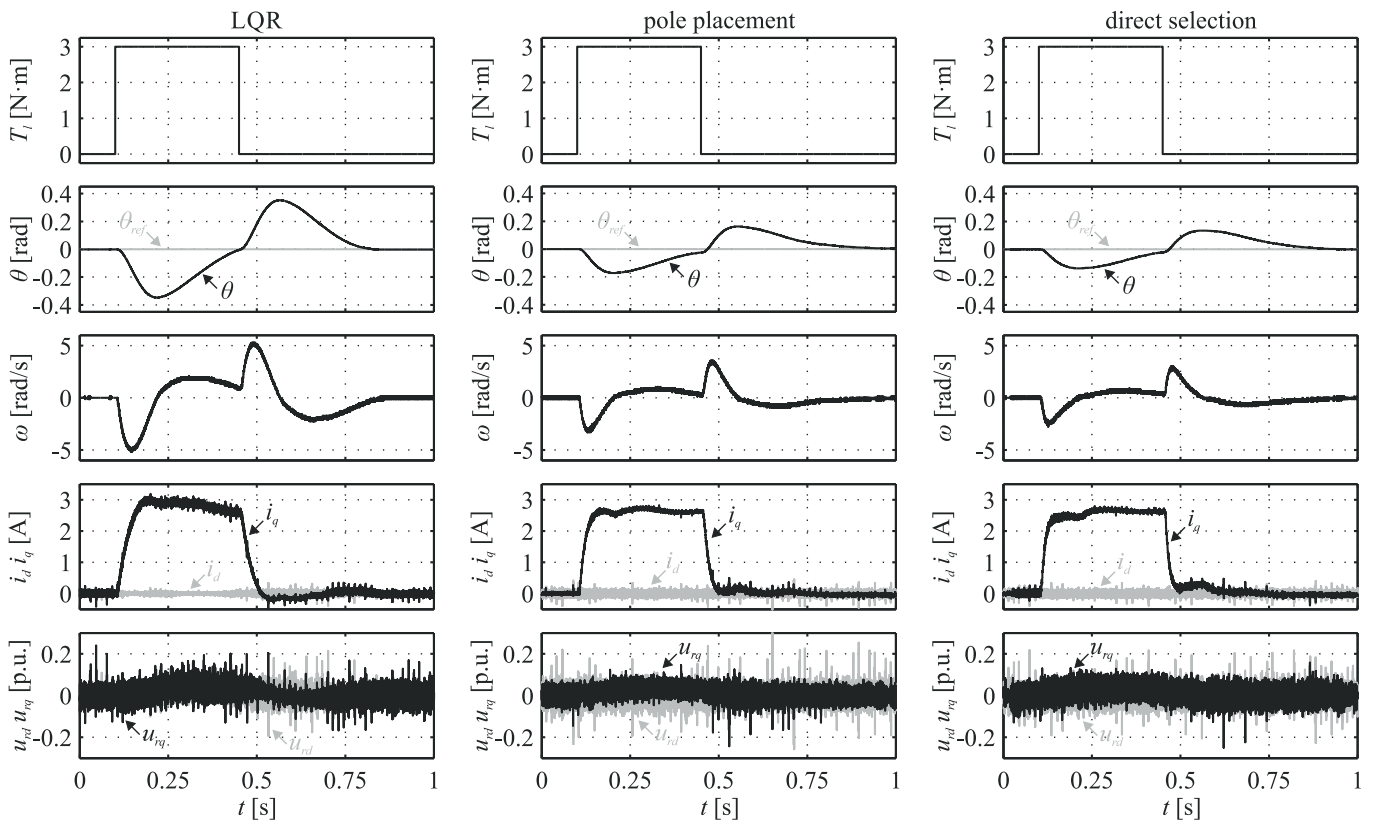


Fig. 11. Experimental responses of PMSM servo-drive to step changes of load torque

Since the load torque compensation is an important feature of servo-drive, it was also examined and obtained results are shown in Fig. 11. It can be seen that good load torque compen-

sation is obtained regardless of method applied for tuning. As it was mentioned earlier, feedforward coefficient remains constant in all cases. Due to this the quality of compensation depends on

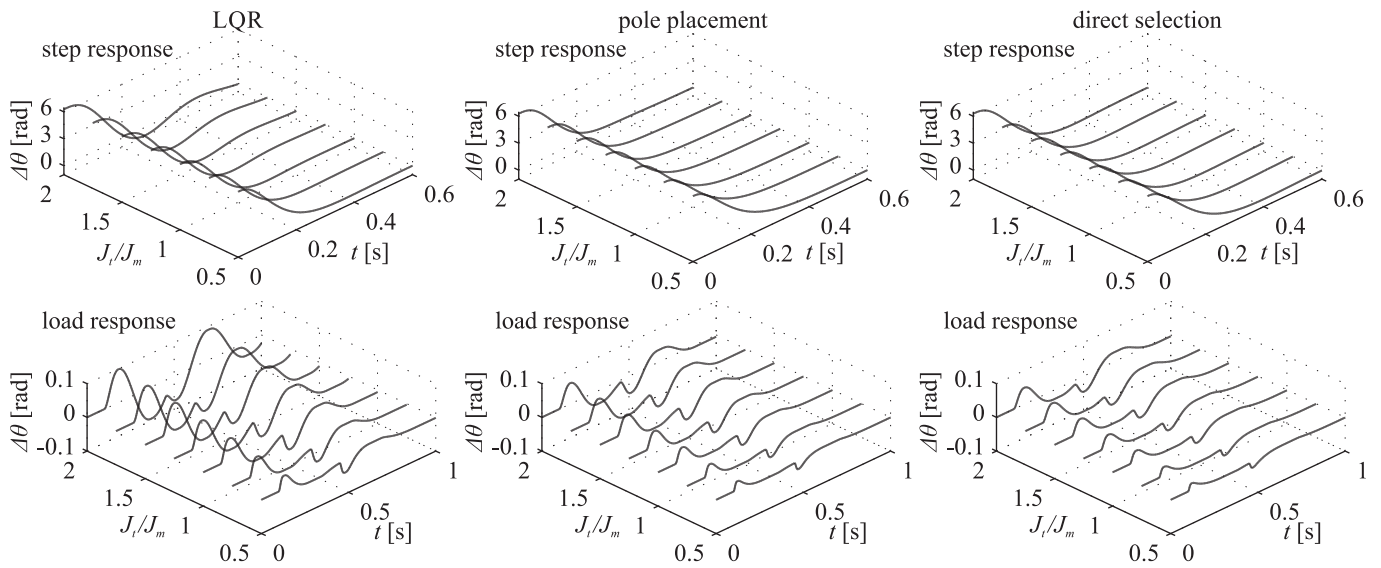


Fig. 12. Experimental responses of PMSM servo-drive to step changes of load torque

automatically selected SFC coefficients. The best load torque compensation is observed for directly selected coefficients of SFC, which is related to the highest value of k_3 in comparison to other methods (i.e. LQR and pole placement). On the other hand, lower values of SFC's coefficients are desirable due to implementation in VSI where reinforcement of unwanted harmonics in voltages and currents may decrease the overall performance of servo-drive. It should be noted that the impact of load torque step changes on position error during tuning is negligible since a much higher value of the position error is caused by the step change of the reference position (see a bottom row in Fig. 8). In order to achieve a better load torque compensation a more complex performance index (e.g. with weighted components) should be introduced [17].

4.3. Robustness. Finally, robustness of designed SFC against moment of inertia changes has been investigated. It is worth noting that tuning of controller was made for nominal value of J_m while simulation studies were accomplished for $J_t \in [0.5 \times J_m; 2 \times J_m]$. From the obtained results shown in Fig. 12 one may conclude that the best robustness against moment of inertia changes has been obtained for SFC with directly selected coefficients. In the case of LQR approach, an overshoot of the step response increases and the load torque compensation decreases for the higher value of J_m .

As robustness indicator, the performance index I_{ABC} (12) has been used and its value obtained for three analysed tuning methods regarding moment of inertia changes is shown in Fig. 13a for step changes of the reference position and in Fig. 13b for step changes of the load torque. From the obtained results it can be concluded that SFCs with coefficients selected directly and with pole placement technique are the most robust against moment of inertia variations. A much worse tolerance against considered changes has been achieved for linear-quadratic optimization. The reason is related to the impact of the integration path and the value of k_3 coefficient.

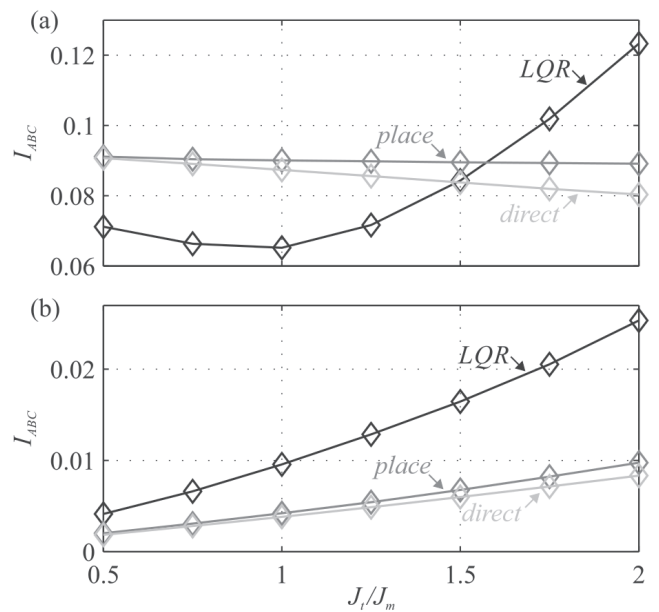


Fig. 13. The performance index I_{ABC} against variable moment inertia for: (a) step response, (b) load response of the PMSM servo-drive

5. Conclusions

This paper presents the efficiency analysis of tuning applied for state feedback controller coefficients. Designed controller has been employed to control mechanical variables in modern PMSM servo-drive. As a result the following conclusions can be drawn:

- Thanks to ABC based tuning, state feedback controller equipped with constraints handling method may be used in motion control applications.
- Since computational complexity of proposed control scheme is relatively low, constrained SFC along with a classical PI current control loop and Luenberger observer

may be implemented in a modern SiC based VSI with high switching frequency to assure efficient and quiet operation of servo-drive.

- The most repeatable results, the lowest value of performance index and the best dynamical behaviour for step response are obtained for linear-quadratic optimization method.
- The load torque compensation and robustness decreases if controller coefficients are lower.

On the basis of conducted studies our recommendation is to use the linear-quadratic optimization method in tuning procedure if no-load or constant-load operation of the servo-drive with well-known parameters is planned. To achieve good disturbance compensation, also for parameters mismatch, a direct selection of controller coefficients is recommended if relatively high values of controller coefficients are acceptable. Finally, it is worth noting that only half of the results obtained for pole placement technique meets requirements related to limitation of the q -axis current. To solve this issue a wider area for poles location should be defined.

Acknowledgements. This research was supported by the basic research fund of the Institute of Engineering and Technology, Nicolaus Copernicus University, Poland.

REFERENCES

- [1] J. Staszak, K. Ludwinek, Z. Gawęcki, J. Kurkiewicz, T. Bekier, and M. Jaśkiewicz, "Utilization of permanent magnet synchronous motors in industrial robots", *2015 International Conference on Information and Digital Technologies*, Zilina, 2015, pp. 342–347, doi: 10.1109/DT.2015.7222995.
- [2] K. Pietrusiewicz, "Multi-degree of freedom robust control of the CNC XY table PMSM-based feed-drive module", *Archives of Electrical Engineering* 61 (1), 15–31 (2012).
- [3] B. Broel-Plater and K. Jaroszewski, "Improving the quality of the classic servo drive by modifying the motion control algorithm," *2017 22nd International Conference on Methods and Models in Automation and Robotics (MMAR)*, Miedzyzdroje, 2017, pp. 43–46, doi: 10.1109/MMAR.2017.8046795.
- [4] S. Brock, D. Łuczak, T. Pajchrowski, and K. Zawirski, "Selected methods for a robust control of direct drive with a multi-mass mechanical load", in: J. Kabziński, ed., *Advanced Control of Electrical Drives and Power Electronic Converters, Studies in Systems, Decision and Control*, Springer, 75–98 (2017).
- [5] K. Urbanski, "A new sensorless speed control structure for PMSM using reference model", *Bull. Pol. Ac.: Tech.* 65 (4), 489–496 (2017).
- [6] K. Dąbala and M. P. Kazmierkowski, "Converter-fed electric vehicle (car) drives—a critical review", *Przegląd Elektrotechniczny* 95 (9), 1–12 (2019).
- [7] L. Jarzebowicz, "Errors of a Linear Current Approximation in High-Speed PMSM Drives", *IEEE Trans. on Power Electron.* 32 (11), 8254–8257 (2017).
- [8] A.R. Ghafari-Kashani, J. Faiz, and M.J. Yazdanpanah, "Integration of non-linear H_∞ and sliding mode control techniques for motion control of a permanent magnet synchronous motor", *IET Electric Power Applications* 4 (4), 267–280 (2010).
- [9] Z. Yin, L. Gong, C. Du, J. Liu and, Y. Zhong, "Integrated Position and Speed Loops Under Sliding-Mode Control Optimized by Differential Evolution Algorithm for PMSM Drives", *IEEE Trans. Pow. Electron.* 34 (9), 8994–9005 (2019).
- [10] K.A. Abuhasel, F.F.M. El-Sousy, M.F. El-Naggar, and A. Abu-Siada, "Adaptive RCMAC Neural Network Dynamic Surface Control for Permanent-Magnet Synchronous Motors Driven Two-Axis X-Y Table", *IEEE Access* 7, 38068–38084 (2019).
- [11] S. Mandra, K. Galkowski, E. Rogers, A. Rauh, and H. Aschemann, "Performance-Enhanced Robust Iterative Learning Control With Experimental Application to PMSM Position Tracking", *IEEE Trans. Control Syst. Technol.* 27 (4), 1813–1819 (2019).
- [12] M. Brasel, "A gain-scheduled multivariable LQR controller for permanent magnet synchronous motor", *2014 19th International Conference on Methods and Models in Automation and Robotics (MMAR)*, Miedzyzdroje, 2014, pp. 722–725, doi: 10.1109/MMAR.2014.6957443.
- [13] M. Safonov and M. Athans, "Gain and phase margin for multi-loop LQG regulators", *IEEE Trans. Autom. Control* 22 (2), 173–179 (1977).
- [14] T. Tarczewski, M. Skiwski, L.J. Niewiara, and L.M. Grzesiak, "High-performance PMSM servo-drive with constrained state feedback position controller", *Bull. Pol. Ac.: Tech* 66 (1), 49–58 (2018).
- [15] A. Apte, V. Joshi, H. Mehta, and R. Walambe, "Disturbance Observer based Sensorless Control of PMSM using Integral State Feedback Controller", *IEEE Trans. Pow. Electron.* 35 (6), 6082–6090 (2020), doi: 10.1109/TPEL.2019.2949921.
- [16] S. Carriere, S. Caux, and M. Fadel, "Optimised speed control in state space for PMSM direct drives", *IET El. Pow. Applicat.* 4 (3), 158–168 (2010).
- [17] K. Paponpen and M. Konghirun, "LQR state feedback controller based on particle swarm optimization for IPMSM drive system", *2015 IEEE 10th Conference on Industrial Electronics and Applications (ICIEA)*, Auckland, 2015, pp. 1175–1180, doi: 10.1109/ICIEA.2015.7334285.
- [18] I. Robandi, K. Nishimori, R. Nishimura, and N. Ishihara, "Optimal feedback control design using genetic algorithm in multi-machine power system", *Int. J. Elect. Power Energy Syst.* 23 (4), 263–271 (2001).
- [19] T. Tarczewski, M. Skiwski, L.M. Grzesiak, and M. Zielinski, "Constrained state feedback control of PMSM servo-drive", *Przegląd Elektrotechniczny* 94 (3), 99–105 (2018).
- [20] M. I. Solihin, Wahyudi, A. Legowo and R. Akmeliawati, "Comparison of LQR and PSO-based state feedback controller for tracking control of a flexible link manipulator", *2010 2nd IEEE International Conference on Information Management and Engineering*, Chengdu, 2010, pp. 354–358, doi: 10.1109/ICIME.2010.5477850.
- [21] T. Tarczewski, L.J. Niewiara, and L.M. Grzesiak, "Auto-tuning of state feedback position controller for PMSM servo-drive – the efficiency analysis", in *Proc. SENE Conf.*, 2019.
- [22] K. Drózdź, M. Kamiński, P.J. Serkies, and K. Szabat, "Application of neural networks for state variables estimation if drive with permanent magnet synchronous motor", *Scientific Papers of The Institute of Electrical Machines, Drives and Measurements of the Wrocław University of Science and Technology Series: Studies and Research* 69 (33), 132–140 (2013).

- [23] L. Harnefors H.-P. and Nee, “Model-Based Current Control of AC Machines Using the Internal Model Control Method”, *IEEE Trans. Ind. Appl.* 34 (1), 133–141 (1998).
- [24] H.-B. Shin and J.-G. Park, “Anti-windup PID controller with integral state predictor for variable-speed motor drives”, *IEEE Trans. Ind. Electron.* 59 (3), 1509–1516 (2012).
- [25] M. Kamiński, “Application of the BAT algorithm in optimization of adaptive state space controller used for two-mass system”, *Przełąd Elektrotechniczny* 93 (1), 300–304 (2017).
- [26] K. Jezernik and M. Rodic, “High precision motion control of servo drives”, *IEEE Trans. Ind. Electron.* 56 (10), 3810–3816 (2009).
- [27] D.C. Lee, S.K. Sul, and M.H. Park, “High performance current regulator for a field-oriented controlled induction motor drive”, *IEEE Trans. Ind. Appl.* 30 (5), 1247–1257 (1994).
- [28] J. Kabziński, P. Mosiołek, and M. Jastrzębski, “Adaptive Position Tracking with Hard Constraints – Barrier Lyapunov Functions Approach”, in: Kabziński J. (eds) *Advanced Control of Electrical Drives and Power Electronic Converters. Studies in Systems, Decision and Control*, vol. 75, Springer, Cham (2017).
- [29] J. Kabziński and P. Mosiołek, “Adaptive control of motion with hard constraints, based on nonlinear state transformation”, *Bull. Pol. Ac.: Tech.* 68 (5), (2020).
- [30] Kim Mun-Soo et al., “A robust control of permanent magnet synchronous motor using load torque estimation”, *ISIE 2001. 2001 IEEE International Symposium on Industrial Electronics Proceedings (Cat. No.01TH8570)*, Pusan, South Korea, 2001, pp. 1157–1162 vol. 2, doi: 10.1109/ISIE.2001.931642.
- [31] R. Szczepanski, T. Tarczewski, K. Erwinski, and L.M. Grzesiak, “Comparison of Constraint-handling Techniques Used in Artificial Bee Colony Algorithm for Auto-Tuning of State Feedback Speed Controller for PMSM”, in *Proceedings of the 15th International Conference on Informatics in Control, Automation and Robotics – Volume 2: ICINCO*, 2018, pp. 269–276, doi: 10.5220/0006904002790286.
- [32] D. Karaboga and B. Basturk, “On the performance of artificial bee colony (ABC) algorithm”, *Appl. Soft. Comput.* 8 (1), 687–697 (2008).
- [33] T. Tarczewski, M. Skiwski, L.M. Grzesiak, and M. Zieliński, “PMSM Servo-Drive Fed by SiC MOSFETs Based VSI”, *Power Electronics and Drives* 3 (1), 35–45 (2018).